JOURNAL OF SPACECRAFT AND ROCKETS
Vol. 39, No. 6, November–December 2002

Electric Propulsion Plasma Simulations and Influence on Spacecraft Charging

M. Tajmar*
ARC Seibersdorf Research, GmbH, A-2444 Seibersdorf, Austria

Electric propulsion thrusters are gaining increasing importance for both commercial applications, as well as for scientific and interplanetary spacecraft, due to their high specific impulse, thrust controllability, and proven reliability. However, because these types of thrusters emit charged propellant, contamination due to collision processes inside the beam and influence on spacecraft charging is a serious issue. Specifically, low-energy charge-exchange ions that can be attracted by potentials on the spacecraft surface need to be well studied. Several three-dimensional particle-in-cell numerical models were developed to study Hall, ion, and field emission thrusters covering both high- and low-thrust electric propulsion systems. The various model approaches and different potential solution implementations (Poisson solver, quasi-neutral plasma assumption) are discussed, depending on the type of thruster simulated. To investigate the effect of the various kinds of thrusters on spacecraft charging, a model is derived linking backflow currents and charge-exchange plasmas with ambient plasma conditions and the spacecraft's floating potential. Simulations suggest that, because backflow currents are very low for field emission thrusters, a dedicated neutralizer is not always necessary to maintain the spacecraft floating potential, especially in low Earth orbits or in combination with a hollow cathode from an ion or Hall thruster.

Nomenclature

A_{SC}, A_{ram}	=	spacecraft and ram area, m^2
e	=	electric charge, 1.602×10^{-19} C
I_i, I_e, I_E, I_B, I_N	=	ion, electron, emission, backflow, and neutralizer current, A
k	=	Boltzmann constant, 1.381×10^{-23} JK^{-1}
m_i	=	ion mass, kg
$n_{e\infty}$	=	electron density in infinity, m^{-3}
n_i, n_e, n_{CEX}	=	ion, electron, and charge-exchange density, m^{-3}
n_∞	=	ambient plasma density, m^{-3}
T_e, $T_{e\infty}$, T_{CEX}	=	electron, ambient electron, and charge-exchange plasma temperature, K
V_f, V_{CEX}	=	spacecraft floating and charge-exchange plasma potential, V
v_{SC}	=	spacecraft relative velocity, ms^{-1}
ϕ	=	potential, V

Introduction

ELECTRIC propulsion thrusters are now being used for many different spacecraft applications, such as interplanetary, telecommunication, or scientific satellites.[1] According to mission requirements, high-, medium-, and low-thrust engines are being developed. For example, a Hall thruster will fly as the primary propulsion system on the European moon satellite[2] SMART-1 (up to 88 mN), the ARTEMIS[3] telecommunication satellite is equipped with ion thrusters (20 mN), and MICROSCOPE[4] will use a field emission electric propulsion (FEEP) thruster (100 μN) for precise attitude control.

In addition to neutral propellant, electric propulsion thrusters emit a plasma that can interact with the spacecraft or the ambient plasma. The main interaction is caused by low-velocity charge-exchange ions, produced inside the plume from collisions between fast beam ions and propellant neutrals. These ions can flow back to the spacecraft surface causing sputtering and inducing an additional current, or can distribute around the spacecraft, which can influence plasma instrument observations. Because of chamber wall and rest gas density limitations, computer particle simulations, verified by ground and in-flight measurements, provide the best means to address this problem.

Because electric propulsion thrusters change the plasma environment around the spacecraft, they will influence the spacecraft's floating potential. Until now, no comparison has been published addressing the influence and differences of spacecraft charging for all electrostatic thrusters (Hall, ion, and FEEP) in different plasma environments. This paper descibes a simple model using backflow currents and ambient plasma environments to compute the spacecraft's floating potential using three-dimensional particle-in-cell (PIC) numerical simulations. This PIC code was validated with available experimental data for all types of thrusters using virtual plasma sensors with real physical dimensions.[5–10] Monte Carlo collisions are used to predict charge-exchange ions and to estimate the amount of current flowing back to the spacecraft. The reader is referred to Refs. 5–10 for any details about the model and simulation parameters used. The thrusters modeled are presently under development or investigation in Europe. Plasma simulation for most of them is rare compared to U.S. technology (for example, Wang et al.,[11] VanGuilder et al.,[12] and references therein). The present paper shall contribute to more European efforts in this area.

Physical Models

Hall and Ion Thrusters

A Hall thruster emits an ion beam out of a ring-shaped anode with a half-cone divergence of about 40 deg. Ion thrusters accelerate the propellant through a grid having a lower half-cone divergence angle of around 10–15 deg. Typical operating parameters are summarized in Table 1. A schematic is shown in Fig. 1. Electrons from an external cathode act as a neutralizer, creating a quasi-neutral plasma. Although the propellant efficiency for these types of thrusters exceed 95%, the neutral density is comparable to the beam ion density due to the much lower thermal velocities (400 m/s) compared to the ion velocities gained due to the acceleration potential of 300–1100 V (20,800–40,000 m/s) between anode and cathode. Moreover, part of the propellant is directed through the cathode, thus providing an additional flow of neutral propellant. Up to 20% of the ions are found to be doubly charged.

A consistent formalism between thrust, ion velocities, and mass flow rates could be established that defines the conditions at the exit

Received 19 October 2001; revision received 12 March 2002; accepted for publication 13 March 2002.

*Research Scientist, Space Propulsion; also Lecturer, Aerospace Engineering Department, Vienna University of Technology, A-2444 Vienna, Austria; martin.tajmar@arcs.ac.at. Member AIAA.

Table 1 Hall and ion thruster performance parameters

Parameter	SPT-100	UK-10	RIT-10
Thrust, mN	84	25	15
Voltage, V	300	1100	1000
Mass flow rate, mg/s	5.6	0.8	0.4
Total efficiency,%	51	77	71
Divergence angle, deg	42	12	11
Outer diameter, mm	100	100	100
Inner diameter, mm	56	——	——

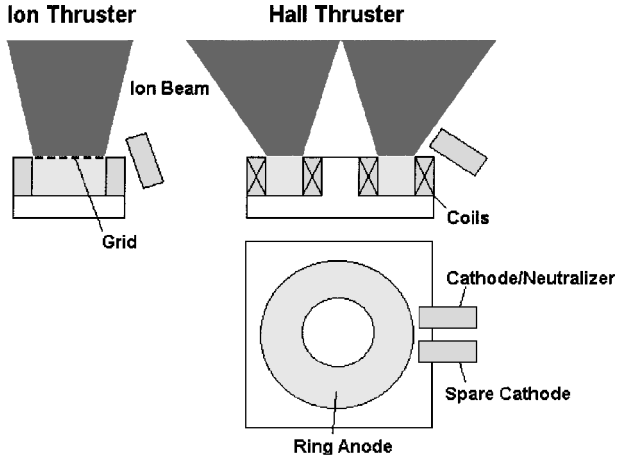

Fig. 1 Hall and ion thruster schematic.

plane of the thrusters.[7] Ion distributions are either homogenous (Hall thruster) or Gaussian (ion thruster), matching ground-testing data.

Because these types of thrusters emit a quasi-neutral plasma, the electrons can be modeled as a fluid, speeding up simulation time. Under the assumption of a collisionless plasma, a constant electron temperature T_e, and a Boltzmann distribution of the electrons, the space charge potential ϕ can be calculated quickly using only ion densities:

$$n_i \approx n_e = n_{e\infty} \times \exp(e\phi/k_B T_e) \tag{1}$$

where $n_{e\infty}$ is calculated using exit potential measurements.

FEEP Thrusters

Two types of FEEP thrusters are currently under development: one using a slit-shaped emitter and cesium as propellant[13] and a needle-type emitter using indium as propellant.[14] A schematic of both thrusters is shown in Fig. 2. Performance data are summarized in Table 2.

A potential difference on the order of 6–12 kV is applied between the emitter and accelerator electrode, creating a focused ion beam squeezed inside a cosine distribution. An important difference between the two designs is that, in the slit configuration, the accelerator electrode is negative (a few kilovolts) with respect to ground, whereas in the needle design the accelerator is on ground potential. Typical divergence angles are between 20 and 60 deg depending on the thrust level.

Cesium, like all alkali metals, has a very high vapor pressure of 2×10^{-4} Pa at the melting point of 28.6°C. Moreover, a high atomic neutral flux of about 1% of the ion flux was observed,[15] suggesting dissociations of microdroplets that are emitted related to the efficiency of the thruster. This flux, together with thermal epavoration (approximately two order below the flux), creates a considerable atomic neutral environment in front of a Cs-FEEP thruster that can cause charge-exchange ions.[9]

Indium has a very low vapor pressure of only 5×10^{-11} Pa at the melting point of 156.8°C. Contribution from thermal evaporation to atomic neutrals is, therefore, neglectible. Only sputtering from the fast beam ions on the microdroplets is considered as an additional source of atomic neutrals. A volumetric production rate based on cross section, sputter yields, ion, and microdroplet measurements was implemented for this case.[5] A separate neutralizer is needed to provide the electrons to keep the spacecraft potential constant.[16] Unlike Hall and ion thrusters, the electrons are not needed to maintain ion emission.

Table 2 Micro Newton FEEP thruster performance parameters

Parameter	Cs-FEEP	In-FEEP
Thrust, μN	580	28
Emitter voltage, kV	6.5	7
Accelerator voltage	−5 kV	0 V
Current, mA	5	0.25
Divergence angle	66 deg perpendicular to slit 20 deg parallel to slit	50 deg

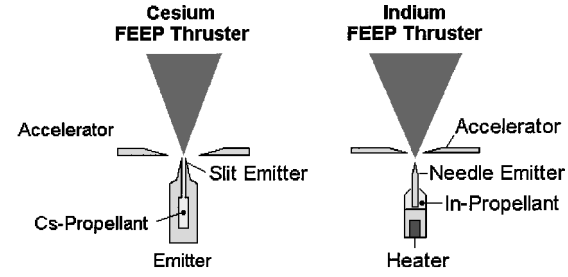

Fig. 2 FEEP Thruster schematic showing a cut through the emitters and accelerator electrode.

Floating Potential Model

Submerged in an ambient plasma environment, the spacecraft will charge up to a floating potential such that the electron and ion currents will balance. Because of the operation of an electric propulsion thruster, the plasma environment will be modified significantly, and, thus, the floating potential will change. In reality, many complex phenomena contribute to spacecraft charging, such as secondary electron emission or photoelectron emission. Also, ambient plasmas are not constant but are influenced, for example, by solar activity. By assuming typical ambient plasma conditions (only one ambient species for simplification), we can estimate spacecraft floating potentials to a reasonable extent and investigate the influence due to the operation of electric propulsion thrusters.

The total ion current from the environment to the spacecraft consists of the thermal flux and a ram component, depending on the spacecraft velocity v_{SC}. In addition, the thruster will emit a current I_E, and charge-exchange ions that flow back to the surface will contribute with the backflow current I_B. We can summarize the total ion current to the spacecraft as

$$I_i = (en_\infty/4) \times \sqrt{8k_B T_{e\infty}/\pi m_i} \times A_{SC} + en_\infty v_{SC} A_{ram} + I_B - I_E \tag{2}$$

where m_i is the ambient ion mass. We can do the same for the total electron current, which also consists of a thermal flux (we assume an ambient potential of 0 V), the current emitted by the neutralizer I_N, and electrons that are flowing from the charge-exchange plasma toward the spacecraft surface:

$$I_e = -\frac{en_\infty}{4} \times \sqrt{\frac{8k_B T_{e\infty}}{\pi m_e}} \times A_{SC} \times \exp\left(\frac{eV_f}{k_B T_{e\infty}}\right) + \iint_{SC} \frac{en_{CEX}}{4} \times \sqrt{\frac{8k_B T_{CEX}}{\pi m_e}} \times \exp\left[\frac{e(V_f - V_{CEX})}{k_B T_{CEX}}\right] dA + I_N \tag{3}$$

where the exponential factor comes, again, from a Boltzmann energy distribution assumption. The charge-exchange parameters are the result of the computer simulation. By setting $I_i + I_e = 0$, we can then derive the spacecraft floating potential V_f by a numerical equation solver.

Numerical Model

A three-dimensional PIC code with Monte Carlo collisions[17,18] was developed. For Hall and ion thrusters, ions and neutrals are

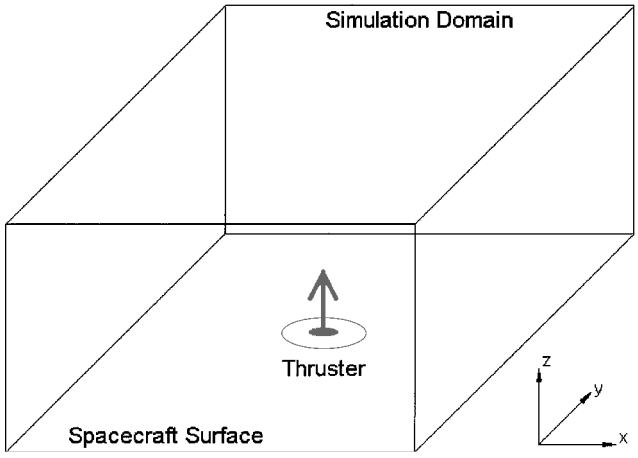

Fig. 3 Simulation domain showing the thruster position in the middle of the bottom plane.

treated as computer particles (one computer particle represents X real atoms), and the potential is computed from Eq. (1), assuming a quasi-neutral plasma. FEEP thrusters emit an ion beam from a point or slit and, therefore, have very high localized plasma densities.[8] The quasi-neutral plasma assumption cannot, therefore, be applied, and the potential has to be solved using Poisson's equation on every gridpoint inside the simulation domain. A successive overelaxation solver has been implemented for this purpose. Because of the absence of space charge (very small emission currents), and because a neutralizer does not change the potential distribution noticeably, no electrons were simulated for FEEP thrusters. Gridpoints and the number of particles were varied and found not to influence the computational results. For details, the reader is referred to the references describing the model.[5–10]

The thruster is modeled on top of the spacecraft surface as illustrated in Fig. 3. The grid size is limited by the debye length of the ambient plasma, and the simulation domain is restricted by available computational resources. For Hall and ion thruster simulations, up to 1,500,000 particles in a $2 \times 2 \times 2$ m domain and $100 \times 100 \times 100$ gridpoints can be calculated on a standard personal computer workstation. Because FEEP thrusters require additional time to solve the potential, only 300,000 particles in a $0.1 \times 0.1 \times 0.1$ domain and up to $40 \times 40 \times 40$ gridpoints can be simulated. Under these circumstances, the computational time to reach equilibrium is about one day.

Plasma Simulations

All electric propulsion simulations presented have been validated using available beam profile and potential measurements.[7,9] In this paper, we will only concentrate on charge-exchange plasma environments, distribution of backflow currents, and influence on spacecraft charging. Therefore, we first assess the plasma environment around each type of thruster, which will be the input for our spacecraft charging calculations. All density plots are evaluated through the middle of the thrusters.

Hall Thruster

The ring-type emission of the stationary plasma thruster (SPT)-100 Hall thruster causes a maximum ion density in the center, at a distance of about 20 cm above the thruster exit plane (Fig. 4). According to our quasi-neutral plasma assumption in Eq. (1), the potential distribution will follow this trend, also forming a potential hump in front of the thruster. The neutral density shows a clear asymmetry due to the propellant flowing through the neutralizer cathode (Fig. 5). Combining Figs. 4 and 5, we expect most of the charge-exchange to be produced close to the thruster exit plane. The potential hump at a distance of 20 cm will reflect those ions back to the surface that were created just below it. Moreover, the positive potential from the ring-type ion emission will focus them in between. We can see this in the charge-exchange ion distribution shown in Fig. 6.

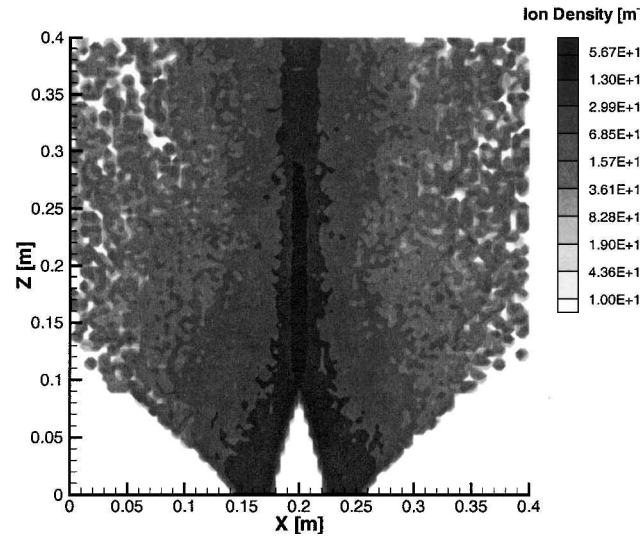

Fig. 4 SPT-100 beam ion density in X–Z coordinates at $Y = 0.2$ m (anode ring emission).

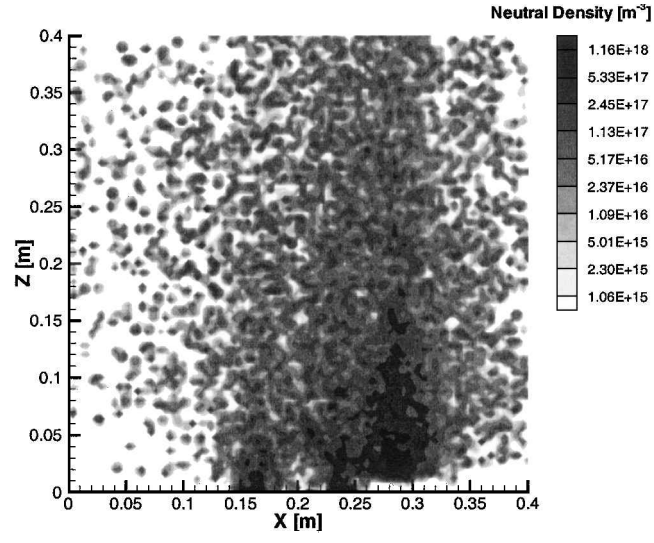

Fig. 5 SPT-100 neutral density in X–Z coordinates at $Y = 0.2$ m (anode ring emission and neutralizer cathode emission).

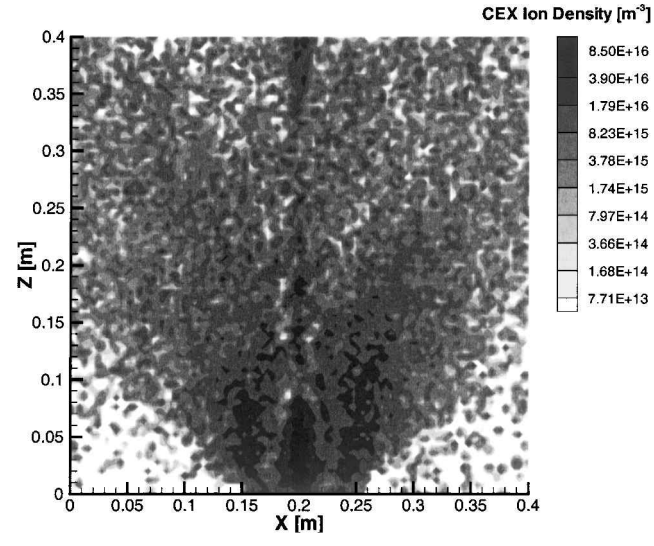

Fig. 6 SPT-100 CEX ion density in X–Z coordinates at $Y = 0.2$ m.

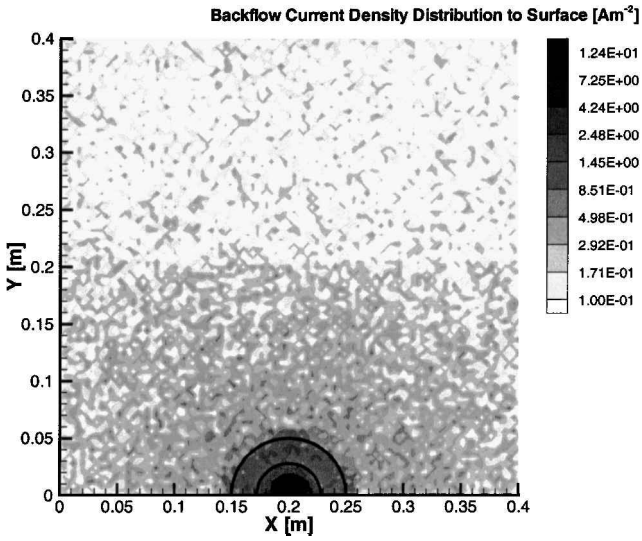

Fig. 7 SPT-100 backflow current distribution in X–Y coordinates at $Z = 0$ m. (Black half-circles indicate anode ring.)

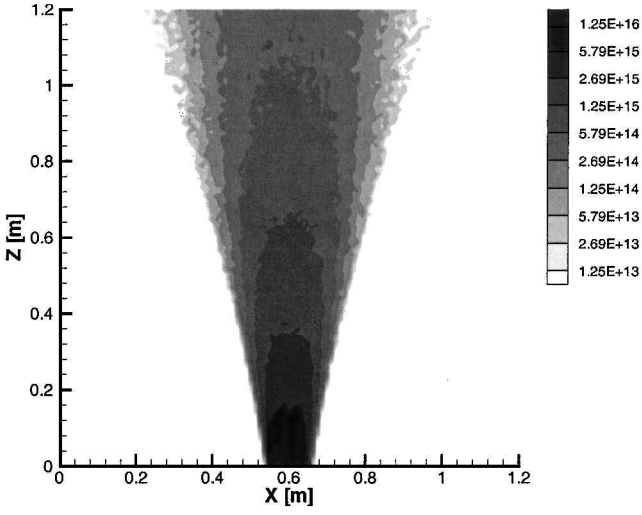

Fig. 8 UK-10 beam ion density in X–Z coordinates at $Y = 0.6$ m.

The backflow current distribution to the surface in Fig. 7 shows a clear maximum of current collected between the anode ring and a slight asymmetry around the anode due to the cathode neutral propellant flow. The charge-exchange ion density that covers the spacecraft structure is only from about one to two orders of magnitude below the beam ion density provided. Because electrons keep this plasma quasi neutral as well, a significant amount of electrons can interact with the spacecraft, similar to a plasma contractor. As we will see later, this effect will greatly reduce spacecraft floating potentials.

Ion Thruster

Contrary to ring-shaped anode of Hall thrusters, ion thrusters emit a circle-area-shaped ion beam and do not cause a potential hump in front of the exit plane (if enough electrons are provided to form a quasi-neutral plasma, of course). The beam ion densities for the UK-10 and RIT-10 ion thrusters are shown in Figs. 8 and 9 and the neutral densities in Figs. 10 and 11, respectively. The charge-exchange ions are again mostly produced close to the thruster exit plane and are then strongly pushed outward due to the positive space charge from the beam ions themselves (Figs. 12 and 13). This is what creates a substantial charge-exchange environment around the thruster and rather high plasma densities close to the spacecraft surface, again, of from one to two orders of magnitude below the beam plasma densities. Most charge-exchange ions are collected just outside the anode region as shown in Figs. 14 and 15, respectively. We note

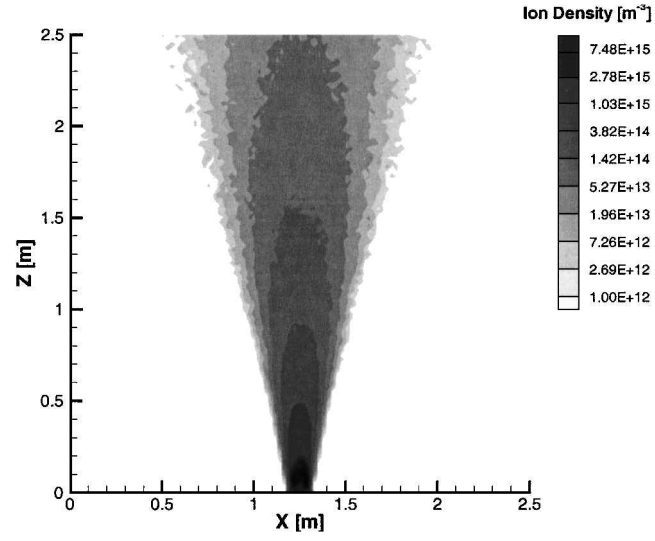

Fig. 9 RIT-10 beam ion density in X–Z coordinates at $Y = 1.25$ m.

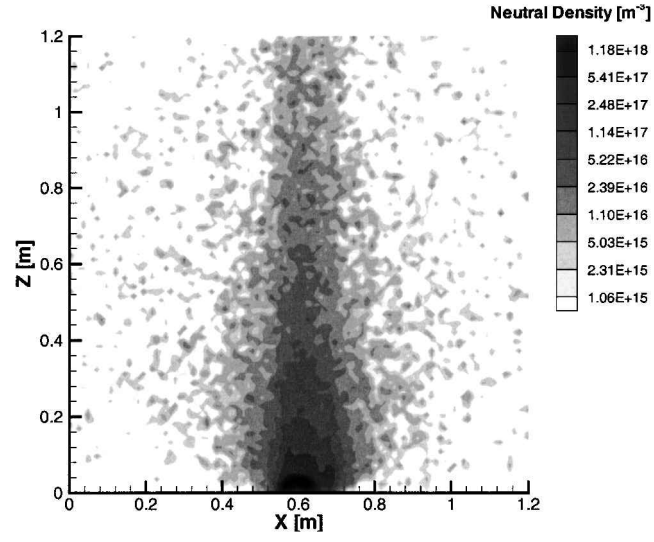

Fig. 10 UK-10 neutral density in X–Z coordinates at $Y = 0.6$ m.

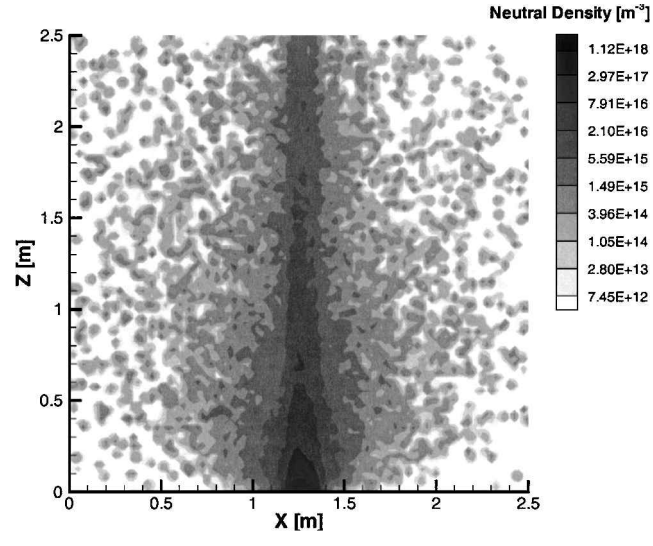

Fig. 11 RIT-10 neutral density in X–Z coordinates at $Y = 1.25$ m.

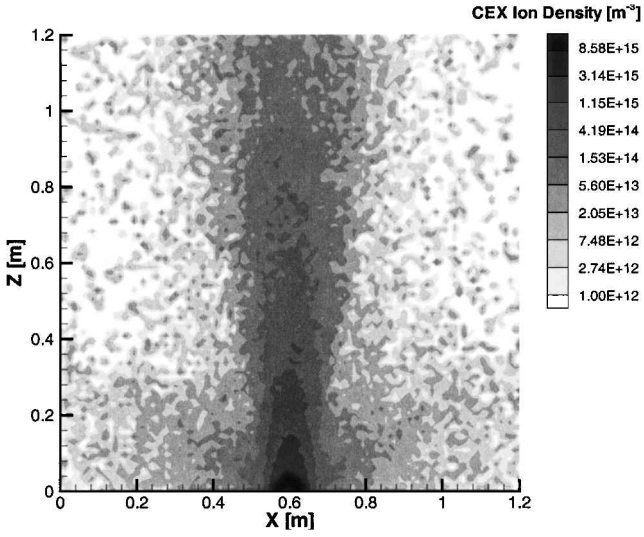

Fig. 12 UK-10 CEX ion density in X–Z coordinates at $Y = 0.6$ m.

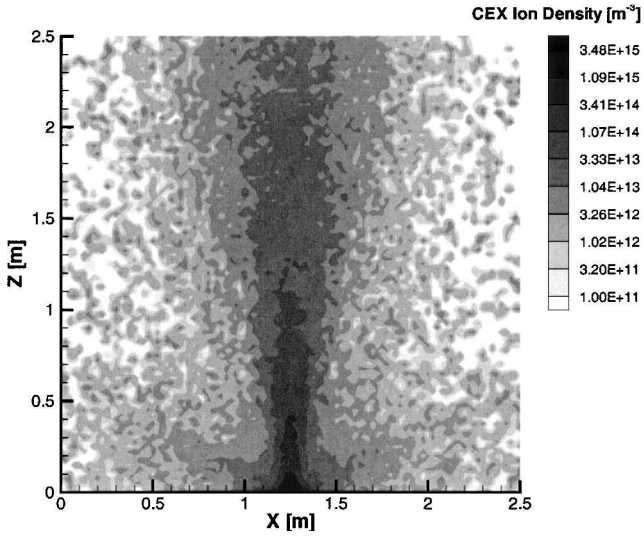

Fig. 13 RIT-10 CEX ion density in X–Z coordinates at $Y = 1.25$ m.

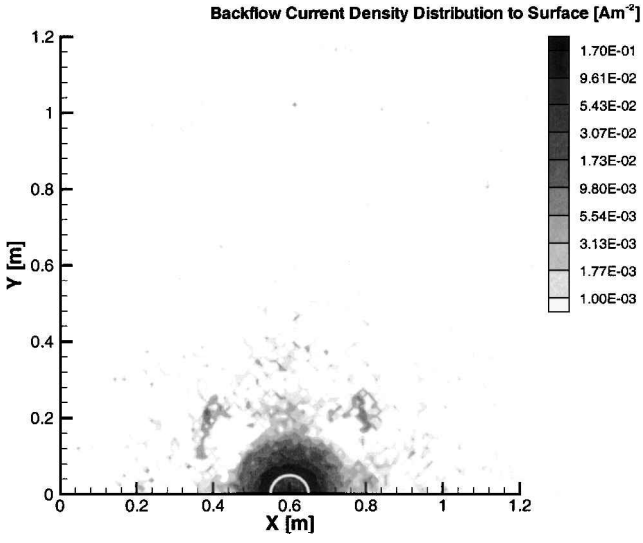

Fig. 14 UK-10 backflow current distribution in X–Z coordinates at $Y = 0.6$ m. (White half-circle indicates thruster outer diameter.)

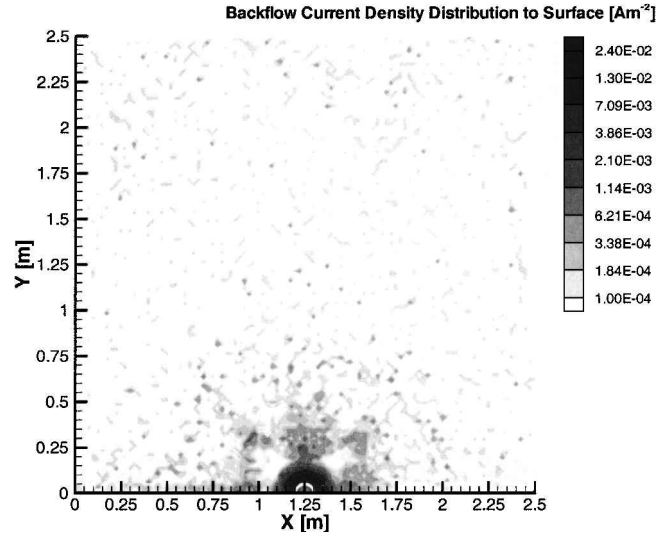

Fig. 15 RIT-10 backflow current distribution density in X–Z coordinates at $Z = 0$ m. (White half-circle indicates thruster outer diameter.)

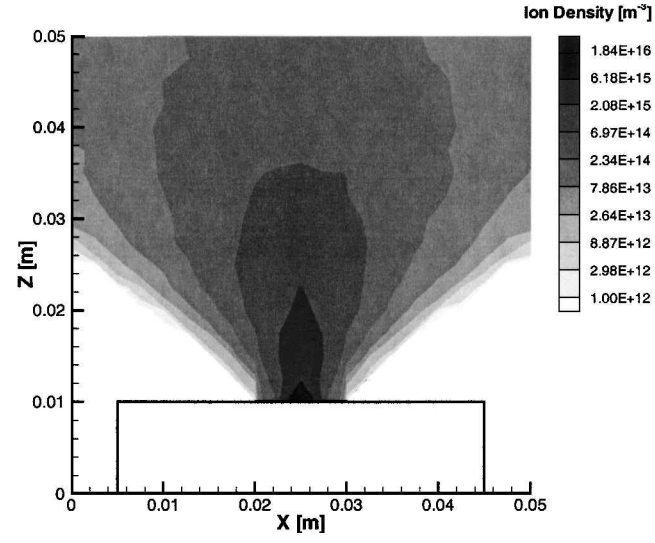

Fig. 16 Cs-FEEP beam ion density in X–Z coordinates at $Y = 0.025$ m on top of spacecraft structure.

again a slight asymmetry due to the neutral propellant flow through the neutralizer cathode.

FEEP Thruster

Cesium FEEP

FEEP thrusters, in general, have a much larger ion beam divergence than Hall or ion thrusters due to their very small acceleration path of only <1 mm compared to many centimeters for the others. That is also why the simulation domain and the grid spacing are much smaller than for Hall and ion thrusters. The beam ion density for a Cs-FEEP thruster is shown in Fig. 16. As discussed in the physical model, cesium has a very high vapor pressure. Combined with the dissociation of microdroplets, the neutral density is even slightly higher then the beam ion density shown in Fig. 17. However, the slit geometry causes very high localized densities. The charge-exchange ions are repelled from the positive space charge and distributed around the thruster, which causes rather low densities. The charge-exchange ion distribution is shown in Fig. 18. Because FEEP thrusters use liquid metal as propellant, the backflowing ions will stick to the surface. This is different from Hall and ion thrusters, where xenon ions only collect electrons to become neutral and are free to leave the surface again.

The backflow distribution of these ions is shown in Fig. 19. The negatively biased accelerator electrode tends to collect most

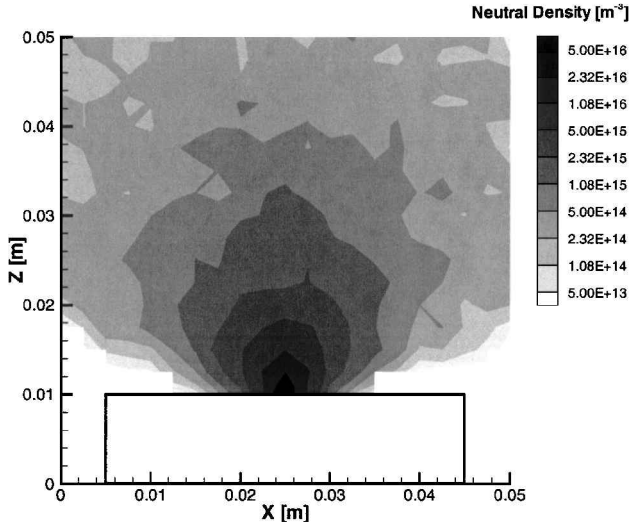

Fig. 17 Cs-FEEP neutral density in X–Z coordinates at $Y = 0.025$ m on top of spacecraft structure.

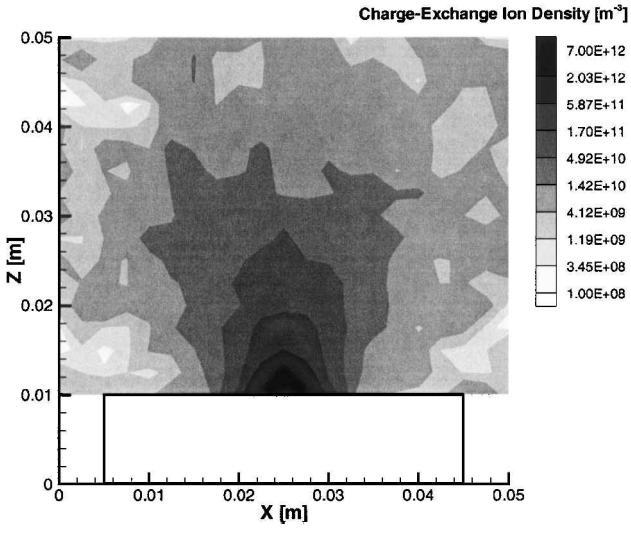

Fig. 18 Cs-FEEP CEX ion density in X–Z coordinates at $Y = 0.025$ m on top of spacecraft structure.

charge-exchange ions, whereas the positive emitter slit repels them. This what forms a characteristic valley distribution shape. Even though the backflow ions initially cover the surface, the high vapor pressure causes rapid thermal evaporation that causes an additional neutral environment that is not treated within this simulation.

Indium FEEP

Beam ion and neutral densities for an In-FEEP thruster are shown in Figs. 20 and 21, respectively. Although ion densities between cesium and indium thrusters are quite comparable, the indium neutral environment is more that six orders of magnitude below that of cesium due to the much lower vapor pressure. This what causes a very low charge-exchange ion environment, 10 orders of magnitude below beam ion densities (Fig. 22). The positive emitter potential dominates the ion backflow distribution shown in Fig. 23. However, because the accelerator electrode is grounded in this case, much fewer charge-exchange ions are attracted to the surface.

In general, FEEP thrusters cause much fewer space charge potentials due to their lower emission currents compared to Hall and ion thrusters. FEEP neutralizers using thermionic cathodes with an anode acceleration potential or field emission arrays (FEA) cathodes[10] have initial energies on the order of 100 to several hundred electron

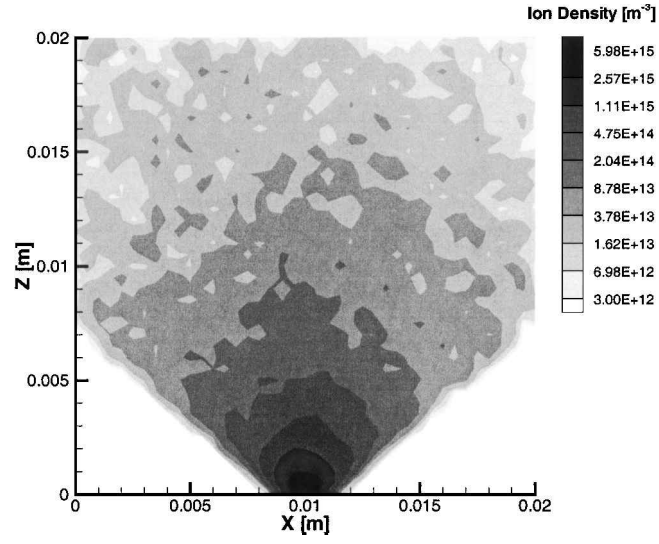

Fig. 20 In-FEEP beam ion density in X–Z coordinates at $Y = 0.01$ m.

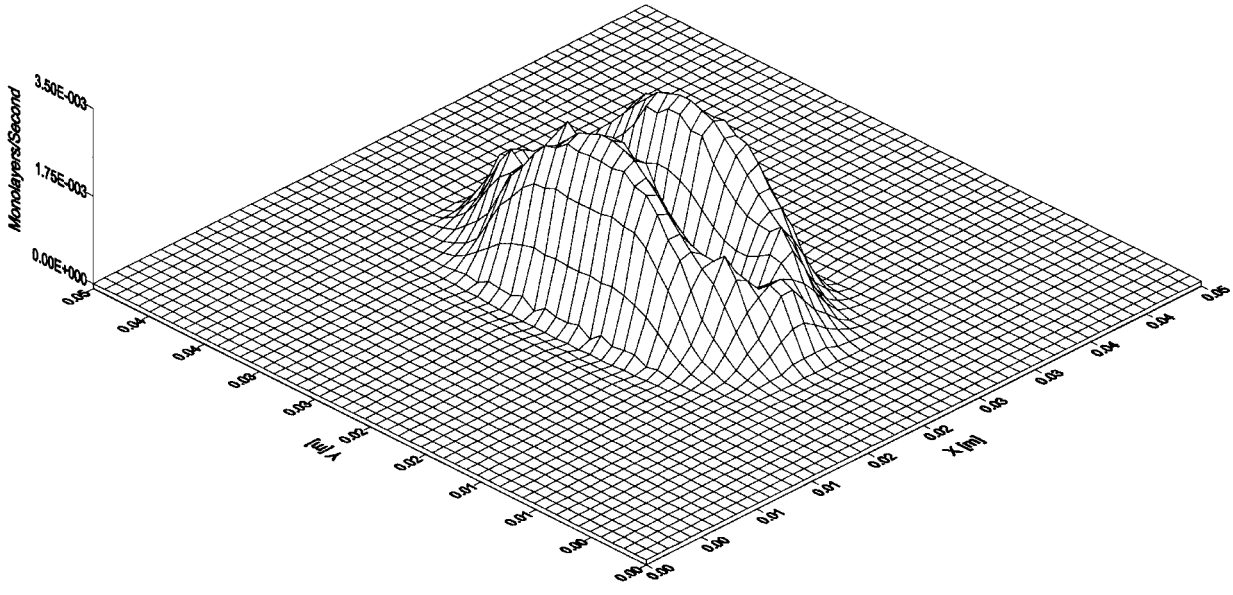

Fig. 19 Cs-FEEP backflow monolayer distribution toward spacecraft surface.

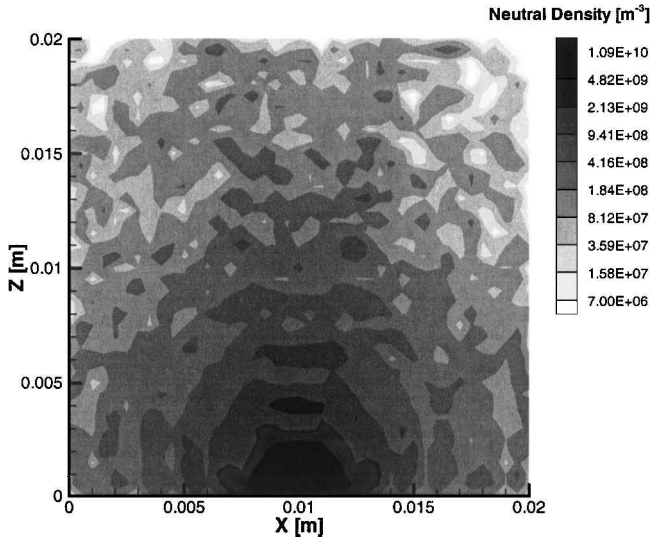

Fig. 21 In-FEEP neutral density in X–Z coordinates at $Y = 0.01$ m.

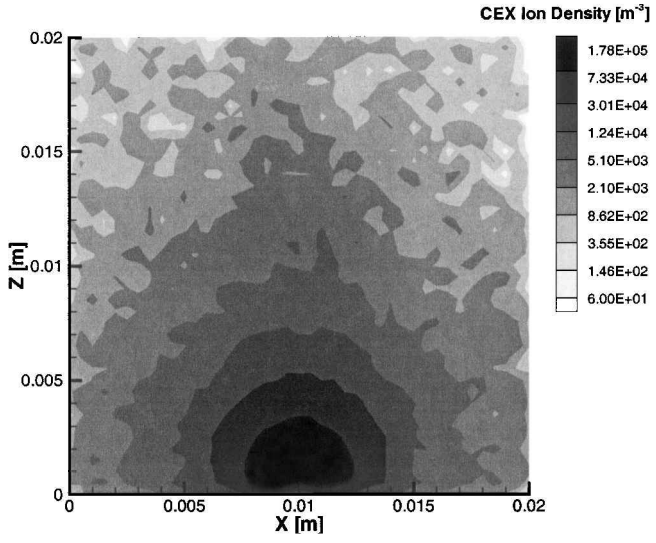

Fig. 22 In-FEEP CEX ion density in X–Z coordinates at $Y = 0.01$ m.

volts and, hence, do not see charge-exchange or beam ion space charge potentials. Therefore, FEEP thrusters will not form a quasi-neutral plasma[8] and the charge-exchange plasma will not act as a plasma contractor to lower spacecraft floating potentials.

Backflow and Spacecraft Charging Calculations

The backflow current distribution was integrated along the spacecraft surface as summarized in Table 3 for the various electric propulsion thrusters. The SPT-100 Hall thruster has a backflow to emission current ratio of about 0.8%. The ion thrusters have slightly lower ratios of around 0.2%. This is consistent with backflow predictions for NASA's NSTAR ion thruster.[19] FEEP thrusters have much lower backflow ratios of 2×10^{-2}% for the cesium and only 7×10^{-8}% for the indium FEEP, respectively. This is due to the lower ion and neutral densities produced by the much lower emission currents compared to Hall and ion thrusters, according to a square root behavior of charge-exchange production to emission current.[5,9] Moreover, in the indium-FEEP case, the atomic neutral environment is simply too low to cause significant charge-exchange collisions. Equation (3) is solved to compute the spacecraft floating potential V_f, assuming a cubic spacecraft of $1 \times 1 \times 1$ m moving at orbital velocity of 8 km/s. Also, the ion emission and neutralizer currents are assumed to be equal, which is generally not the case. Three different ambient conditions are evaluated: vacuum, low-Earth-orbit (LEO) and geosynchronous-Earth-orbit (GEO) conditions (parameters summarized in Table 4). All spacecraft floating potentials are shown in Table 5. In all cases, an electron temperature of 1 eV was

Table 3 Backflow currents at typical operating conditions

Thruster	Emission current I_E, mA	Backflow current I_B, mA	I_B/I_E ratio, %
SPT-100	4100	32	0.78
UK-10	440	1.02	0.23
RIT-10	210	0.35	0.16
Cs-FEEP	5	9.3×10^{-4}	1.9×10^{-2}
In-FEEP	0.25	1.8×10^{-10}	7.2×10^{-8}

Table 4 Ambient plasma conditions

Orbit	Plasma density, m^{-3}	Electron temperature, eV	Ambient ion mass, kg
LEO	10^{12}	0.1	2.66×10^{-26}
GEO	10^{6}	1000	1.66×10^{-27}

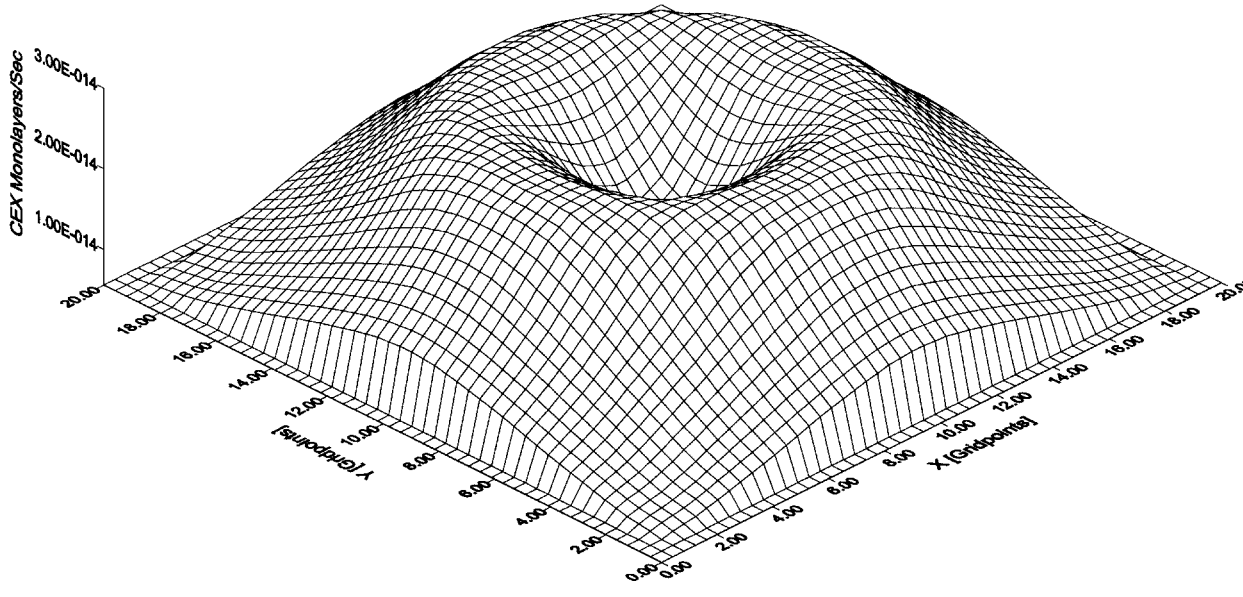

Fig. 23 In-FEEP backflow monolayer distribution toward spacecraft surface.

Table 5 Spacecraft floating potentials at typical electric propulsion operating conditions

	Spacecraft floating potential, V		
Thruster	Vacuum	LEO	GEO
No thruster	0	−0.35	−3744.6
SPT-100	−16.3	−16.2	−16.3
UK-10	−6.5	−5.6	−6.5
RIT-10	−8.9	−7.3	−9.1
Cs-FEEP without neutralizer	——	−0.35	−2645
In-FEEP without neutralizer	——	−0.35	−3744.6

assumed for the charge-exchange plasma, which is lower than the fixed electron temperature in the beam (3–5 eV) due to the lower charge-exchange(CEX) plasma densities.

With no thruster firing, the floating potentials in LEO are slightly different from those in a vacuum, in our case, $V_f = -0.35$ V. Because of the much higher electron temperatures of kiloelectron volts in GEO (solar wind, etc.), the floating potentials can obtain several thousand negative volts. Operating an electric propulsion thruster, the CEX plasma will act as a plasma bridge between the spacecraft surface, the ion beam, and the neutralizer electrons. In that case, the floating potential is reduced from −3744 to −16 V, or even down to −6 V for the Hall and ion thrusters, respectively. The difference between GEO and vacuum thruster operation is negligible due to the already very low plasma densities in GEO of 10^{-6} m^{-3}. Floating potential values of around −10 V have actually been measured in space experiments using ion thrusters on the SCATHA[20] and ATS-6 spacecraft.[21] In the case of LEO conditions, the CEX plasma contact causes a slightly more negative floating potential than the initial −0.35 V, due to the lower ambient electron temperature of only 0.1 eV.

The very low ion and backflow currents from FEEP thrusters do not change the LEO floating potentials due to the relatively high ambient plasma density (the debye length is very small). Unlike Hall and ion thrusters, a FEEP thruster does not need a neutralizer to reduce the space charge necessary for operation. Because the FEEP plasma is not quasi neutral and the neutralizer electrons usually do not couple to the CEX ions,[8] FEEP thrusters do not act as a plasma contactor. This makes it impossible to evaluate the spacecraft floating potential in vacuum because the positive backflow current is not balanced by an electron current flowing to the surface. In reality, electrons will be attracted by changed spacecraft floating potentials to counterbalance this effect. However, due to the limited simulation domain, this effect could not be modeled. Therefore, the GEO floating potential values for FEEP thruster operation are only partially correct, although the ambient plasma can supply electrons and ions in this case.

Because the spacecraft floating potential remains unchanged in LEO with and without thruster operation, a neutralizer for FEEP thrusters is not always necessary to maintain the spacecraft floating potential. The ambient ion current (order of tens of milliamperes) is usually at least one order of magnitude higher that the emission current of a FEEP thruster (in our example, 0.25 for In-FEEP and 5 mA for the Cs-FEEP, respectively). Another possible scenario for saving a FEEP neutralizer is a spacecraft using ion or Hall thrusters for high thrusts and FEEP thrusters for precision attitude orbit control. In that case, the CEX plasma from the bigger thrusters also act as a plasma bridge to counterbalance the charging effects from the much smaller FEEP thruster currents. Depending on the spacecraft orbit, spacecraft size, and the number of FEEP and other thrusters at certain thrust levels, the model can be used to predict the change of the spacecraft floating potential. In case of marginal change, the additional neutralizer for FEEP thrusters can be abandoned, saving power, mass, and volume.

Summary

A three-dimensional numerical PIC simulation was developed to model Hall, ion, and FEEP thruster operation onboard a spacecraft. Backflow currents were shown to be below 1% of the emitted current for all thrusters. CEX plasmas produced by Hall and ion thrusters were shown to act similar to a plasma contactor and are able to reduce the spacecraft floating potential significantly, from several thousand negative volts in GEO to around −10 V. FEEP thrusters do not couple electrons to their CEX ions and, hence, are not able to reduce spacecraft floating potentials significantly. Depending on spacecraft, orbits, and additional electric propulsion thrusters, the model suggests that a neutralizer is not always necessary for spacecraft equipped with FEEP thrusters.

References

[1] Saccoccia, G., González del Amo, J., and Estublier, D., "Electric Propulsion: A Key Technology for Space Missions in the New Millennium," *ESA Bulletin*, Vol. 101, Feb. 2000.

[2] Racca, G. D., Foing, B. H., and Rathsman, P., "An Overview on the Status of the SMART-1 Mission," International Academy of Astronautics, Paper IAA-99-IAA.11.2.09, Oct. 1999.

[3] Bassner, H., Berg, H. P., Fetzer, K., and Müller, G., "Ion Propulsion Package IPP for N/S-Stationkeeping of the ARTEMIS Satellite," International Electric Propulsion Conf., Paper IEPC-91-055, Oct. 1991.

[4] Bonnet, J., Marque, J. P., and Ory, M., "Development of a Thrust Balance in the Micronewton Range," *Proceedings of the 3rd International Conference on Spacecraft Propulsion*, ESA, Noordwijk, The Netherlands, 2000, pp. 807, 808.

[5] Tajmar, M., Rüdenauer, F., and Fehringer, M., "Backflow Contamination of Indium Liquid-Metal Ion Emitters (LMIE): Numerical Simulations," International Electric Propulsion Conf., Paper IEPC-99-070, Oct. 1999.

[6] Tajmar, M., Gonzáles, J., and Hilgers, A., "Modeling of Spacecraft–Environment Interactions on SMART-1," *Journal of Spacecraft and Rockets*, Vol. 38, No. 3, 2001, pp. 393–399.

[7] Tajmar, M., Gonzalez, J., Estublier, D., and Saccoccia, G., "Modelling and Experimental Verification of Hall and Ion Thrusters at ESTEC," *Proceedings of the 3rd International Conference on Spacecraft Propulsion*, ESA, Noordwijk, The Netherlands, 2000, pp. 683–691.

[8] Tajmar, M., and Wang, J., "Three-Dimensional Numerical Simulation of Field-Emission-Electric-Propulsion Neutralization," *Journal of Propulsion and Power*, Vol. 16, No. 3, 2000, pp. 536–544.

[9] Tajmar, M., and Wang, J., "Three-Dimensional Numerical Simulation of Field-Emission-Electric-Propulsion Backflow Contamination," *Journal of Spacecraft and Rockets*, Vol. 38, No. 1, 2001, pp. 69–78.

[10] Marrese-Reading, C., Polk, J., Mueller, J., Owens, A., Tajmar, M., Fink, R., and Spindt, C., "In-FEEP Ion Beam Neutralization with Thermionic and Field Emission Cathodes," International Electric Propulsion Conf., Paper IEPC-01-290, Oct. 2001.

[11] Wang, J., Brinza, D. E., Young, D. T., Nordholt, J. E., Polk, J. E., Henry, M. D., Goldstein, R., Hanley, J. J., Lawrence, M. D., and Shappirio, J., "Deep Space One Investigations of Ion Propulsion Plasma Environment," *Journal of Spacecraft and Rockets*, Vol. 37, No. 5, 2000, pp. 545–555.

[12] VanGilder, D. B., Boyd, I. D., and Keidar, M., "Particle Simulations of a Hall Thruster Plume," *Journal of Spacecraft and Rockets*, Vol. 37, No. 1, 2000, pp. 129–136.

[13] Marcuccio, S., Genovese, A., and Andrenucci, M., "Experimental Performance of Field Emission Microthrusters," *Journal of Propulsion and Power*, Vol. 14, No. 5, 1998, pp. 774–781.

[14] Genovese, A., Steiger, W., and Tajmar, M., "Indium FEEP Microthruster: Experimental Characterization in the 1–100 μN Range," AIAA Paper 2001-3788, July 2001.

[15] Mitterauer, J., "Field Emission Electric Propulsion Spectroscopic Investigations on Slit Emitters," Vienna Univ. of Technology, Final Rept. on ESTEC Contract 5051/82/NL/PB (SC), Dec. 1985.

[16] Fehringer, M., Rüdenauer, F., and Steiger, W., "Micronewton Indium Ion Thrusters," International Electric Propulsion Conf., Paper IEPC-99-6, Oct. 1999.

[17] Birdsall, C. K., and Langdon, A. B., *Plasma Physics via Computer Simulation*, Adam Hilger, New York, 1991.

[18] Birdsall, C. K., "Particle-in-Cell Charged-Particle Simulations, Plus Monte Carlo Collisions with Neutral Atoms, PIC-MCC," *IEEE Transactions on Plasma Science*, Vol. 19, No. 2, 1991, pp. 65–85.

[19] Samanta Roy, R. I., Hastings, D. E., and Gatsonis, N. A., "Numerical Study of Spacecraft Contamination and Interactions by Ion-Thruster Effluents," *Journal of Spacecraft and Rockets*, Vol. 33, No. 4, 1996, pp. 535–542.

[20] Craven, P. D., Olsen, R. C., Fennell, J., Croley, D., and Aggson, T., "Potential Modulation on the SCATHA Spacecraft," *Journal of Spacecraft and Rockets*, Vol. 24, 1987, pp. 150–157.

[21] Olsen, R. C., "Modification of Spacecraft Potentials by Plasma Emission," *Journal of Spacecraft and Rockets*, Vol. 18, No. 5, 1981, pp. 462–469.

I. D. Boyd
Associate Editor